

TR-01-1905

AD0753864 3558

ER28791

UNLIMITED

ROYAL AIRCRAFT ESTABLISHMENT
TECHNICAL REPORT 71184

TR 71184

MARCH
1972



Crown Copyright
1972

AD753864

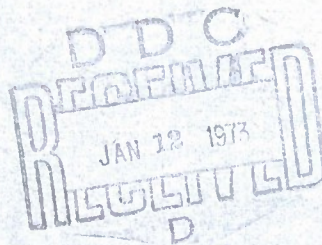
A PROJECTED GRID METHOD FOR
RECORDING THE SHAPE OF
THE HUMAN FACE

by

J. Cobb

3558

20090504 438



PROCUREMENT EXECUTIVE, MINISTRY OF DEFENCE
FARNBOROUGH, HANTS

AD-753864

UDC 578.087 : 611.92 : 526.918 : 614.894

ROYAL AIRCRAFT ESTABLISHMENT

Technical Report 71184

September 1971

A PROJECTED GRID METHOD FOR RECORDING THE SHAPE OF THE HUMAN FACE

by

J. Cobb

SUMMARY

This Report describes the work carried out to design an equipment which would quickly and cheaply record the shapes of a large number of human faces. It is intended for use in an anthropometric survey with a view to providing data for a project aimed at improving the fit and comfort of oxygen masks for Service use. The data will be examined to discover a parameter of the human face which can be used to determine which mask size is best suited to any individual.

A simple, quick and adequately accurate equipment for recording one side of the face has been developed from an earlier design and includes several refinements to simplify the analysis. The survey will assume that the mean aircrew face is symmetrical although it is realised that individual faces are not.

The accuracy of the equipment has been measured and is within the required one millimetre.

Departmental Reference: IR 123



CONTENTS

	<u>Page</u>
1 INTRODUCTION	3
2 BRIEF SURVEY OF METHODS CONSIDERED	3
2.1 Holography	3
2.2 Stereophotogrammetry	4
2.3 First moiré method	5
2.4 Second moiré method	5
3 METHOD EMPLOYED	6
3.1 Basic system	6
3.2 Modifications to basic system	6
3.2.1 'Telecentric lens' arrangement	6
3.2.2 Colour grid	7
3.2.3 Measuring graticule	7
3.3 Accuracy	8
4 CONCLUSION	8
Appendix A Calculations of the errors of the basic system	9
Appendix B Effective magnification in film plane of telecentric system	11
Appendix C Accuracy of telecentric system	15
Appendix D Theoretical inaccuracies of non-telecentric system	16
References	19
Illustrations	Plates 1 & 2
Drgs. 054/900870 to 054/900881	Figures 1-6
Neg. C 8374	Figures A1, B1 & B2, C1-C3, D1 & D2
Detachable abstract cards	-

1 INTRODUCTION

In response to a request from the Human Engineering Division of Engineering Physics Department, RAE, several methods of recording the shape of the human face were investigated, with a view to producing data to be used to design new oxygen masks for RAF aircrew, which would be a good fit, comfortable to wear for long periods, and which would not leak when used for pressure breathing.

The object of the work is not to provide individual masks but to make a small range of mask 'types' or 'sizes', one or other of which will be a reasonable fit on any particular wearer.

The statistical analysis which this implies does not assume that individuals have symmetrical faces but it does assume that particular facial shapes occur with equal frequency on the left and right hand sides of the human face.

Once the mask has been designed, a method of deciding which type or size is best suited to any individual will be needed. Since it is obviously impracticable to measure everyone's face and subject the results to best-fit analysis, some parameter of the face, for example length of nose, width of mouth, distance from bridge of nose to point of chin, etc., will be sought which correlates highly with the size of mask needed. All that will then be necessary to issue the correct mask to any individual will be to measure this parameter with a tape-measure.

The most convenient way to record the shape of an object for later analysis is by a contour map of the surface, and efforts were concentrated on methods which would produce this directly. The requirement was to be able to record the shape of the lower part of the face, from the bridge of the nose downwards, to an accuracy of one millimetre.

2 BRIEF SURVEY OF METHODS CONSIDERED

2.1 Holography

An investigation was carried out into the possibility of recording human faces holographically. Although this does not produce a contour map it does record the three dimensional surface for later measurement. This method was not pursued for various reasons:

- (a) A high power laser is needed to make a hologram of an object the size of the human face if the exposure time is to be kept short. The exposure has to be kept short enough that no part of the object moves

more than about a tenth of a wavelength of light. This means that a flash laser (1-3 joules output energy, single mode, 30 nanoseconds pulse length) must be used and difficulties are then experienced in getting sufficient coherence length¹. The high power of the laser can also be dangerous to the eyes and skin².

(b) It was found experimentally difficult to measure the depth of any part of a reconstruction to an accuracy better than about 2 millimetres. For this test a dummy head was used, a hologram of which could be made with a low power laser and a long exposure time.

2.2 Stereophotogrammetry

This involves the taking of two photographs with matched cameras from different viewpoints and comparing these in a stereo viewer capable of measuring the stereo difference³. In order to provide surface detail on the face to facilitate viewing in stereo, the face was illuminated from the front using a projector with a piece of wire mesh in the slide holder. This produced a bright squared pattern on the face which made the negatives very easy to fuse in the viewer. The exact size and shape of the mesh did not matter since this was not itself being measured but served merely to define the position of the face surface. With a stereo viewer the author found it quite easy to measure spot heights to well within the one millimetre accuracy required, but could not trace out any individual contour, this obviously requiring a skilled operator. However, several commercial organisations specialising in aerial survey would be prepared to carry out the analysis.

In summary, the advantages are as follows:-

- (a) Several companies could carry out the analysis as a matter of course.
- (b) The contour interval can have any value and does not have to be decided at the photography stage. Spot heights can be measured.
- (c) The method covers the whole face in one exposure and is potentially the most accurate of those investigated.

However there are corresponding disadvantages:-

- (d) The equipment for taking the photographs involves two matched cameras with synchronous shutters, or a single camera and a system of mirrors.
- (e) The analysis requires a skilled operator and specialised plotting equipment.

(f) The contours cannot be seen at the time of taking or even at the time of plotting until the plot is complete. This means that an accurate means of positioning the subject's head with reference to supposed 'fixed' points, for example the Frankfurt horizontal³ (a plane defined by the ears and eyes), must be used.

2.3 First moiré method

The next method tried was a form of moiré gauging where the face surface and a reference plane were illuminated at an angle with straight lines, and moiré fringes were formed between the distorted lines on the face and the straight lines on the reference, as in Fig.1.

Fringes did appear but they were of low contrast because this is the additive type of moiré. They appeared only in those places where the brightness of the face surface matched that of the reference, disappearing elsewhere in the high background level of illumination. Therefore this system is not suitable in its simple form.

2.4 Second moiré method

This is a subtractive moiré method which gives high contrast fringes⁴. A point source of light casts a shadow of a coarse grating on the face (Fig.2). The moiré fringes are formed between the distorted shadow as seen from the camera position and the grating itself, illuminated by the light reflected from the face. The fringes are high contrast because this is a subtractive method, and they appear equally well over the whole surface of the face because the brightnesses of the two gratings are automatically equal. In addition it was found⁵ that if the grating were moved in its own plane during the exposure in a direction perpendicular to the lines as in Fig.2, the shadow on the face and the graticule itself both blurred out, but the moiré fringe pattern remained stationary. This much improves the contour definition.

This method suffers from a geometric error in that those parts of the subject which are close to the camera (e.g. the nose) appear larger than they should, and those parts which are farther from the camera (e.g. the ears) appear smaller than they should. Also, in regions of high gradient (e.g. the side of the nose), the contours are close together and difficult to count with certainty.

3 METHOD EMPLOYED

3.1 Basic system

In the basic system a grid of equally spaced, parallel straight lines is projected on to the side of the subject's face, and the result photographed from the front. This is similar to a method previously used in EP Department⁶. Each line on the grid gives rise to a plane of light in the region of the subject. These planes intersect with the surface of the face so that, from the front, the locus of points of equal 'depth' is illuminated by a particular line. Thus a contour map of one half of the face is recorded on the film.

The map is not accurate since the planes of light are not parallel to each other but diverge from the vicinity of the projector lens. The nose will have fewer lines intersecting its depth than it should and the ear will have more, making the nose appear shallower and the ears appear deeper than they really are. Similarly in the photographing side of the system (as in 2.4 above) the nose will produce a larger image than is correct and the ear a smaller one, being farther away.

If we imagine the co-ordinate system of Fig.3 then the inaccuracies arising from these geometrical effects can be calculated as in Appendix A. The result is that if on the photograph a point appears to be at the position (x,y,z) then it will have the correct position (x',y',z')

$$\text{where } x' = x \frac{(1 - z/C)}{(1 - zx/PC)}$$

$$y' = y \frac{(1 - z/C)}{(1 - zx/PC)}$$

$$z' = z \frac{(1 - x/P)}{(1 - zx/PC)}$$

C = distance of camera lens
from centre of system

P = distance of projector lens
from centre of system

It can be seen that if, and only if, $C = P = \infty$ then the equations reduce to $x' = x$, $y' = y$, $z' = z$ and measurements from the photograph will require no correction.

3.2 Modifications to basic system

3.2.1 'Telecentric lens' arrangement

Since it is physically impossible to remove both camera and projector to an infinite distance, this is achieved optically by the use of a type of telecentric system. Positive lenses of diameters greater than the size of

the subject to be measured are placed in the optical paths of the projector and the camera in the region of the subject. The distances of the camera and projector from the subject are adjusted so that their lenses are at the principal focal points of these telecentric lenses.

From the position of the subject, the projector and camera viewed through these lenses both appear to be infinitely distant, thus fulfilling the requirements to produce an accurate contour map. The proof that the effective magnification at the film plane is constant irrespective of the object's position in the system can be seen in Appendix B. The same mathematics applies to the projector system. The telecentric lenses used in the system were twelve inch diameter plano-convex single elements with a focal length of one metre. With the addition of a plane mirror eighteen inches by twelve inches in the projector side to fold the optical path, the whole instrument measures five feet by three feet and provides ample space for a person's head and shoulders while being small enough to be easily transportable. The arrangement can be seen in plan view in Fig.4.

3.2.2 Colour grid

A coloured straight line grid was used instead of the black and white one of Ref.6. This helps to avoid confusion when counting contours in regions where they are close together, such as at the side of the nose and around the lips.

A grid of five colours was employed, each line on the face having a depth of about 2 millimetres, so that each colour appears at depth intervals of 10 millimetres. This means that colour film must be used in the camera but this is a small price to pay for the greatly increased clarity of the final picture (Plate 1). The colours chosen were white plus four others evenly spaced around the CIE colour chart. They were from the Ilford filter range, narrow cut tricolour red, bright spectrum yellow, bright spectrum blue-green and narrow cut tricolour blue. It was found convenient to arrange them in the order white, blue, blue-green, yellow, red, with a narrow black gap between each line (Plate 2). It was also found advisable to light the opposite side of the face with white light as this makes the subject recognisable and the picture easier to view.

3.2.3 Measuring graticule

The question arose of superimposing a graticule on each photograph, so as to record the exact magnification and also to provide convenient measuring points. At first a square graticule was projected on to the front of the face.

In order to avoid distortion due to the different depths of the face, the projector lens used for this purpose must appear coincident with the camera lens, i.e. a partial reflector must be placed in front of the camera. This has several disadvantages, the major ones being loss of light and the introduction of unwanted reflections. These were overcome by putting the beam-splitter round the other way and projecting the graticule straight into the camera. This means that the beam-splitter can have a low reflectivity so that there is very little light loss and in fact a piece of ordinary non-silvered glass proved suitable. There is a slight difficulty in that multiple reflections are seen because of the finite thickness of the glass and the fact that the graticule appears to originate from the distance of the subject, i.e. about four feet. If this distance were made infinite then the multiple images would all overlap; this can be achieved by placing the subject at the other focal point of the photographing telecentric lens. This entails a re-design of the layout but does not greatly increase the overall size of the instrument. The new plan view is seen in Fig.5. Three basic types of graticule used to test the system are shown in Fig.6.

3.3 Accuracy

In order to check the accuracy of the system, a flat test object 30 cm by 20 cm was placed in the object space at an angle of 30° . Thirty five crosses were marked on it at known positions and a photograph was taken with a plate camera. The positions of the crosses in all three dimensions were measured from the plate and compared with the known positions. The rms error in position over the whole volume was found to be 0.66 millimetres. This test volume was almost the maximum it was possible to measure with the apparatus and considerably larger than one side of the human face from bridge of nose to chin. It can be seen that the accuracy is within the requirement of 1 millimetre. The complete analysis can be seen in Appendix C. An analysis of the theoretical inaccuracies involved in using a similar size system without the telecentric lenses and assuming the the 'map' is correct can be seen in Appendix D. The rms error in this case is about 9 millimetres over the same volume.

4 CONCLUSION

The apparatus described provides a simple and convenient method of recording facial contours and is sufficiently easily portable to be taken to sites, such as RAF Stations, for the purpose of carrying out on-the-spot surveys. Subsequent analysis of the recordings can be done centrally.

Appendix A

CALCULATIONS OF THE ERRORS OF THE BASIC SYSTEM

In Fig.A1, point A is a general point of position (x',y',z') . A_C and A_P are the projections of A onto the X-Y plane and Y-Z plane from the points C and P and therefore represent the apparent position of point A, as seen from the Z and X directions respectively.

Let $OX = x$, $OZ' = z'$, $OC = C$, etc.

By similar triangles OYC and CZ'B,

$$\frac{y}{y'} = \frac{C}{C - z'}$$

$$y' = y(1 - z'/C) \quad (1)$$

and similarly

$$x' = x(1 - z'/C) \quad (2)$$

and

$$z' = z(1 - x'/P) \quad (3)$$

Substituting (3) into (2)

$$x' = x \left\{ 1 - \frac{z}{C} (1 - x'/P) \right\}$$

$$PCx' = PCx - Pzx + zx'x$$

$$x'(PC - zx) = x(PC - Pz)$$

$$x' = \frac{x(1 - z/C)}{(1 - zx/PC)} \quad (4)$$

similarly for z

$$z' = \frac{z(1 - x/P)}{(1 - zx/PC)} \quad (5)$$

Substituting (5) into (1)

$$y' = y \left\{ 1 - \frac{z}{C} \frac{(1 - x/P)}{(1 - zx/PC)} \right\}$$

$$y'(1 - zx/PC) = y(1 - zx/PC - z/C + zx/PC)$$

$$y' = \frac{y(1 - z/C)}{(1 - zx/PC)} \quad (6)$$

Equations (4), (5) and (6) are the correction equations needed to find the actual position (x', y', z') of a point from its apparent position (x, y, z) , measured from the centre of the system O.

It can be seen that if, and only if, $C = P = \infty$, then these equations simplify to $x' = x$, $y' = y$, $z' = z$, i.e. measurements taken directly from the photograph give the correct position or size of a point or object in all three dimensions. A telecentric lens system is an optical method of making C and P mathematically infinite while maintaining physically finite dimensions to the equipment.

Appendix B

EFFECTIVE MAGNIFICATION IN FILM PLANE OF TELECENTRIC SYSTEM

From Fig.B1 using the cartesian sign convention, the size on the film plane of the image of an object O can be calculated.

For lens L_1

$$\text{object distance} = -u_1$$

$$\text{image distance} = u_2$$

$$\frac{1}{F_1} = \frac{1}{u_2} - \frac{1}{-u_1}$$

$$u_2 = \frac{F_1 u_1}{u_1 - F_1}$$

Provided $u_1 > F_1$, u_2 is negative and the image of O formed by L_1 is virtual in the object space.

For lens L_2 , the physical object distance $|F_1| + |u_2|$ is therefore given by $(F_1 - u_2)$ from which, applying the sign convention,

$$\text{object distance} = -(F_1 - u_2) = \frac{F_1^2}{u_1 - F_1}$$

$$\text{image distance} = v$$

$$\frac{1}{F_2} = \frac{1}{v} - \frac{u_1 - F_1}{F_1^2}$$

$$v = \frac{F_1^2 F_2}{F_1^2 - F_1 F_2 + F_2 u_1} \quad (7)$$

Primary magnification = d'/d

$$d'/d = u_2/u_1 = \frac{F_1}{u_1 - F_1}$$

Secondary magnification = d''/d'

$$\frac{d''}{d'} = \frac{V}{u_2 - F_1} = \frac{V(u_1 - F_1)}{F_1^2}$$

$$\frac{d''}{d'} = \frac{F_2(u_1 - F_1)}{F_1^2 - F_1F_2 + F_2u_1}$$

Overall magnification = $d''/d = (d''/d')(d'/d)$

$$\frac{d''}{d} = \frac{F_1F_2}{F_1^2 - F_1F_2 + F_2u_1} \quad (8)$$

$$\text{Now } \tan \alpha = \frac{d''}{V} = \frac{F_1F_2d}{(F_1^2 - F_1F_2 + F_2u_1)} \cdot \frac{(F_1^2 - F_1F_2 + F_2u_1)}{F_1^2F_2} \text{ from (7) and (8)}$$

From which

$$\tan \alpha = \frac{d}{F_1} \quad (9)$$

and is independent of u_1 , the original object position.

Suppose now a photographic plate or film is inserted in a specific position, so defining a recording plane (Fig.B1). The image on that film may or may not be in focus, but its size (KP'') is clearly still proportional to $\tan \alpha$ and is consequently independent of u_1 by equation (9). In this sense, therefore, the 'magnification' of the image in a predetermined plane is constant and independent of the location of the object. The telecentric system thus behaves quite differently from a conventional photographic objective in this respect.

Changes in object positions do, however, affect image sharpness in the usual way. Suppose that in Fig.B2 plane X is the fixed recording plane and that planes Y and Z are the focussed image planes corresponding to extreme axial movements of the object in either direction beyond which lack of image sharpness in the recording plane X ceases to be tolerable. Take the limiting

'circle of confusion' in either case to have the conventional value of $V/1000$. Then, by similar triangles

$$\left. \begin{aligned} \frac{A}{V - \Delta V_y} &= \frac{V}{1000\Delta V_y} \\ \frac{A}{V - \Delta V_z} &= \frac{V}{1000\Delta V_z} \end{aligned} \right\}$$

or

$$\left. \begin{aligned} \Delta V_y &= \frac{V^2}{1000A + V} \\ \Delta V_z &= \frac{V^2}{1000A - V} \end{aligned} \right\}$$

where A is the physical aperture of the camera lens.

Here, ΔV_y and ΔV_x are the inner and outer depths of focus of the system as conventionally defined. They may be approximately related to the corresponding depths of field Δu_{1y} and Δu_{1z} by differentiating equation (7) above, when

$$\begin{aligned} \Delta u_1 &\simeq -(F_1^2 - F_1 F_2 + F_2 u_1)^2 \Delta V \\ &\simeq -F_1^2 / V^2 \cdot \Delta V \end{aligned}$$

from which

$$\left. \begin{aligned} \Delta u_{1y} &\simeq -\frac{F_1^2}{1000A + V} \\ \Delta u_{1z} &\simeq -\frac{F_1^2}{1000A - V} \end{aligned} \right\} \quad (10)$$

From equations (10), taking typical values for the various quantities,

$$\left. \begin{aligned} F_1 &= 100 \text{ cm} \\ F_2 &= 5 \text{ cm} \\ A &= 1 \text{ cm} \\ u_1 &= 30 \text{ cm} \end{aligned} \right\}$$

- (i.e. using an f/5 camera system) - it is obvious that $V \approx F_2$ in equations (10) and

$$\Delta u_{1y} \approx \Delta u_{1z} \approx \frac{-F_1^2}{1000A} = -10 \text{ cm}$$

Such a system therefore has a total depth of field of about 20 cm, which is plainly adequate to cope with an object of the axial depth of a human face.

Appendix CACCURACY OF TELECENTRIC SYSTEM

The test object shown in Fig.C2, when viewed at an angle of 30° as in Fig.C1, should appear to be a series of rectangles 50 millimetres high and $(50 \cos 30^\circ)$ millimetres wide. The depth interval should be $(50 \sin 30^\circ)$ millimetres. The test object was photographed on a 5×4 plate and the positions of the 35 image points measured in the vertical and lateral directions. Their depths were found by counting the contours between them.

With a knowledge of the correct positions of the points as described above, the best estimates of magnification on the plate and of contour intervals can be obtained from the mean separations of the points on the plate, lens aberrations being ignored. The individual distances of the points on the plate from the centre of the pattern can now be divided by the magnification, resulting in a table of 35 positions representing the apparent positions of the test points according to the telecentric optical system. These positions were then subtracted from the known positions producing an error chart. This can be seen in Table C3. The four corners were not measurable as they were outside the diameter of the telecentric lens and so were not visible.

It can be seen that the errors are well within the tolerance of 1 millimetre required except at the extreme edges of the field. The root-mean-square errors in each of the three dimensions were as follows,

$$\text{rms X error} = 0.54 \text{ mm}$$

$$\text{rms Y error} = 0.32 \text{ mm}$$

$$\text{rms Z error} = 0.21 \text{ mm.}$$

This gives an overall rms error of the position of a point in space of 0.66 millimetre. This is over the surface of an object covering a width of 260 millimetres, a height of 200 millimetres and a depth of 150 millimetres.

Appendix D

THEORETICAL INACCURACIES OF NON-TELECENTRIC SYSTEM

In Fig.D1, let $OP = P = 1$ metre, $OC = C = 1$ metre, $OX = x$, $OZ' = z'$, $OA = a$, etc. AOB is the test chart. x' is the correct X-value of the point A, X is its apparent position viewed from the camera lens C.

$$\text{Error in X-value} = (x' - x)$$

In triangle OAX by sine rule

$$\frac{a}{\sin(90 + \alpha)} = \frac{x}{\sin(60 - \alpha)}$$

Using $\tan \alpha = x/C = x$ (in metres)

$$x = \frac{\sqrt{3}a}{2 + a}$$

In triangle OAX'

$$x' = \frac{\sqrt{3}a}{2}$$

$$\text{X-error} = (x' - x) = \frac{\sqrt{3}a^2}{2a + 4} \quad (\text{a in metres})$$

On the test chart a takes the values 0, ± 50 , ± 100 , ± 150 millimetres. These produce a table of X-errors as follows,

10.53, 4.56, 1.11, 0, 1.06, 4.12, 9.06 millimetres.

From these figures can be found the rms X-error = 5.77 millimetres.

In triangle OBZ by sine rule

$$\frac{b}{\sin(90 + \beta)} = \frac{z}{\sin(30 - \beta)}$$

Using $\tan \beta = z/P = z$ (in metres)

$$z = \frac{b}{2 + \sqrt{3}b}$$

In triangle OBZ'

$$z' = b/2$$

$$Z\text{-error} = (z' - z) = \frac{\sqrt{3}b^2}{2\sqrt{3}b + 4} \quad (b \text{ in metres})$$

On the test chart b takes the values 0, ± 50 , ± 100 , ± 150 millimetres. These produce a table of Z-errors as follows,

8.62, 3.98, 1.04, 0, 1.13, 4.75, 11.20 millimetres.

From these figures the rms Z-error is 5.86 millimetres.

In Fig.D2, $DE = y =$ apparent height of point A. Correct height of point A = y' . Lateral position of A on the test chart = x' .

By similar triangles CDE, CFA

$$\frac{y}{y'} = \frac{CD}{CF}$$

In similar triangles COD, CHF

$$\frac{CD}{CF} = \frac{CO}{CH}$$

$$CH = CO + OH = 1 + OF \sin 30^\circ$$

$$CH = 1 + \frac{1}{2}x'$$

Therefore

$$\frac{y}{y'} = \frac{1}{1 + \frac{1}{2}x'}$$

$$Y\text{-error} = (y' - y) = y' \left(1 - \frac{2}{2 + x'} \right)$$

$$(y' - y) = \frac{x'y'}{2 + x'} \quad (x' \text{ and } y' \text{ in metres}).$$

The Y-error therefore depends on both x' and y' .

On the test chart x' takes the values 0, ± 50 , ± 100 , ± 150 millimetres and y' takes the values 0, ± 50 , ± 100 millimetres. These give a table of 35 Y-errors as follows

Y-errors in millimetres

-8.11	-5.26	-2.56	0	2.44	4.76	6.98
-4.05	-2.63	-1.28	0	1.22	2.38	3.49
0	0	0	0	0	0	0
4.05	2.63	1.28	0	-1.22	-2.38	-3.49
8.11	5.26	2.56	0	-2.44	-4.76	-6.98

From this table the rms Y-error is found to be 3.56 millimetres. From these three rms errors an overall rms error in spatial position of 8.96 millimetres can be found.

It can be seen from the three error charts that the error exceeds 1 millimetre for all points beyond about 50 millimetres of the centre. The above figures represent the calculable inaccuracies of the system and the experimental error would increase all these figures slightly.

REFERENCES

- | <u>No.</u> | <u>Author</u> | <u>Title, etc.</u> |
|------------|-------------------------------|--|
| 1 | D. A. Ansley | Techniques for pulsed laser holography of people.
<i>Applied Optics</i> , <u>9</u> , 4, 815-821 (1970) |
| 2 | Ministry of Technology | Laser systems - Code of Practice.
1969 Edition |
| 3 | L. F. H. Beard
P. H. Burke | Evolution of a system of stereophotogrammetry for the study of facial morphology.
<i>Med. and Biol. Illustration</i> , <u>XVII</u> , 1, 20-25 |
| 4 | P. S. Theocaris | <i>Moiré fringes in strain analysis</i> .
Chapter 6, page 219, Edinburgh, Pergamon Press (Scotland) Ltd., (1969) |
| 5 | H. Takasaki | Moiré topography.
<i>Applied Optics</i> , <u>9</u> , 6, 1467-1472 (1970) |
| 6 | E. J. Lovesey | A method for determining facial contours by shadow projection.
RAE Technical Report 66192 (1966) |

Reports quoted are not necessarily available to members of the public or to commercial organisations.

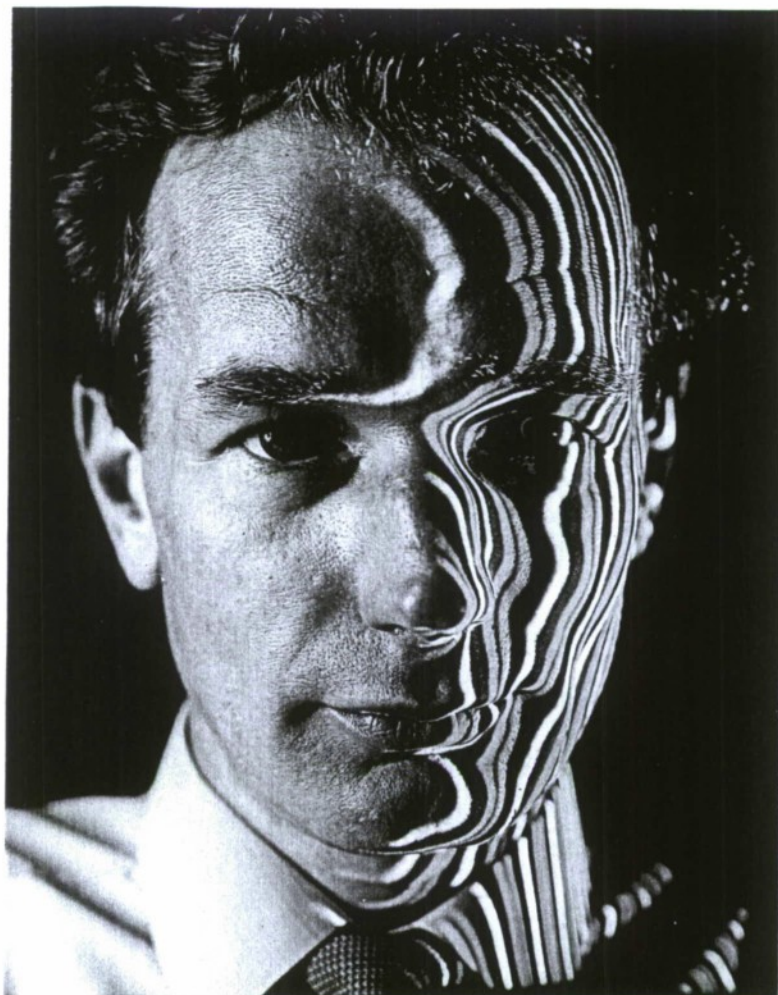


Plate 1

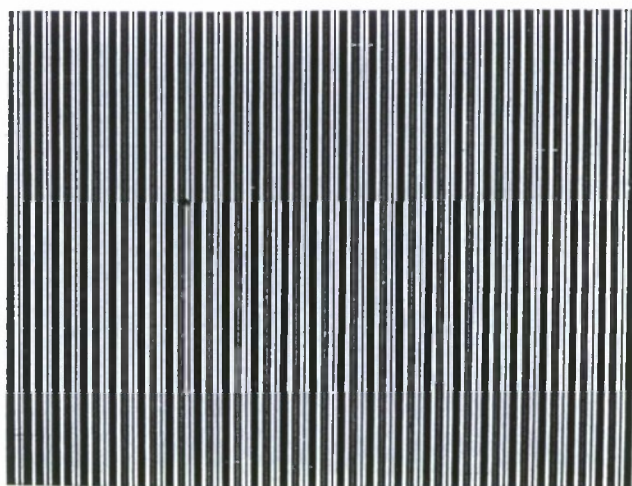
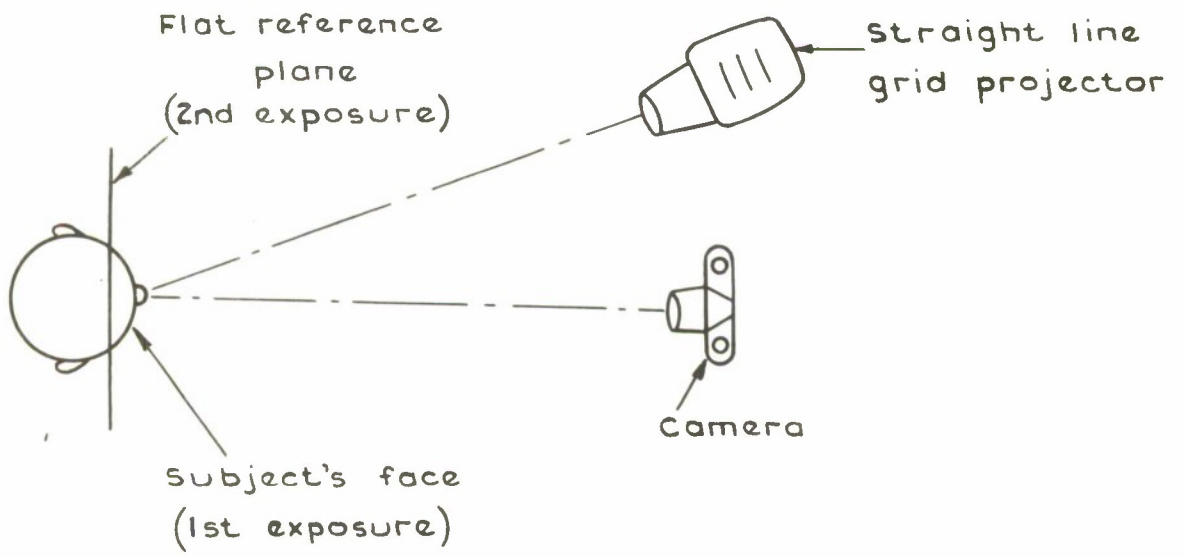


Plate 2



TR 71184

054 900870

Fig.1 First Moiré method

Fig. 2

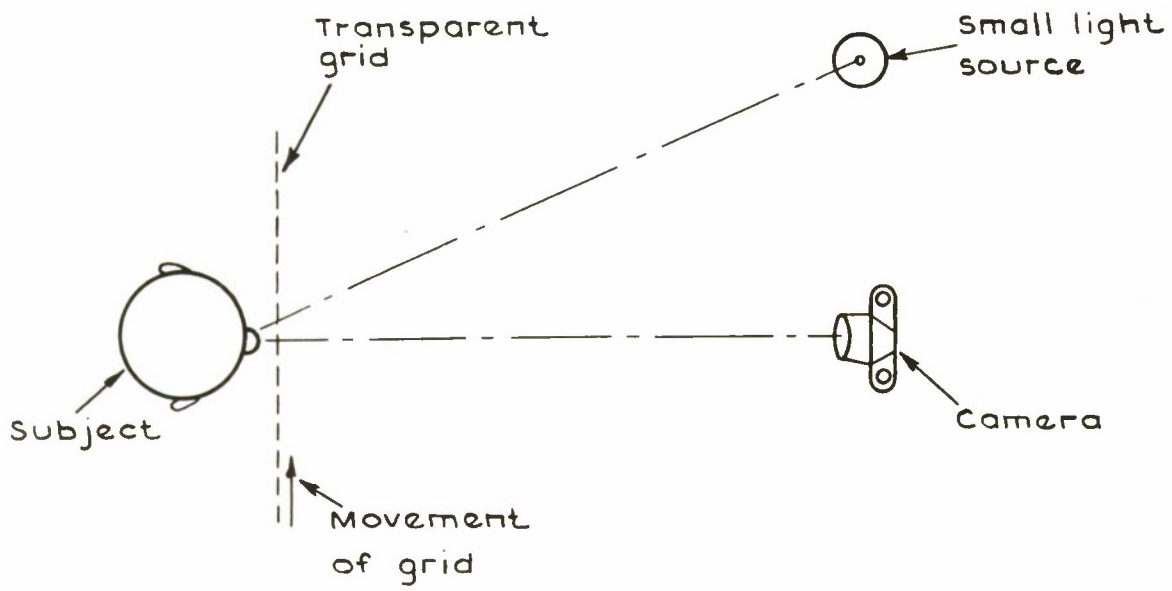
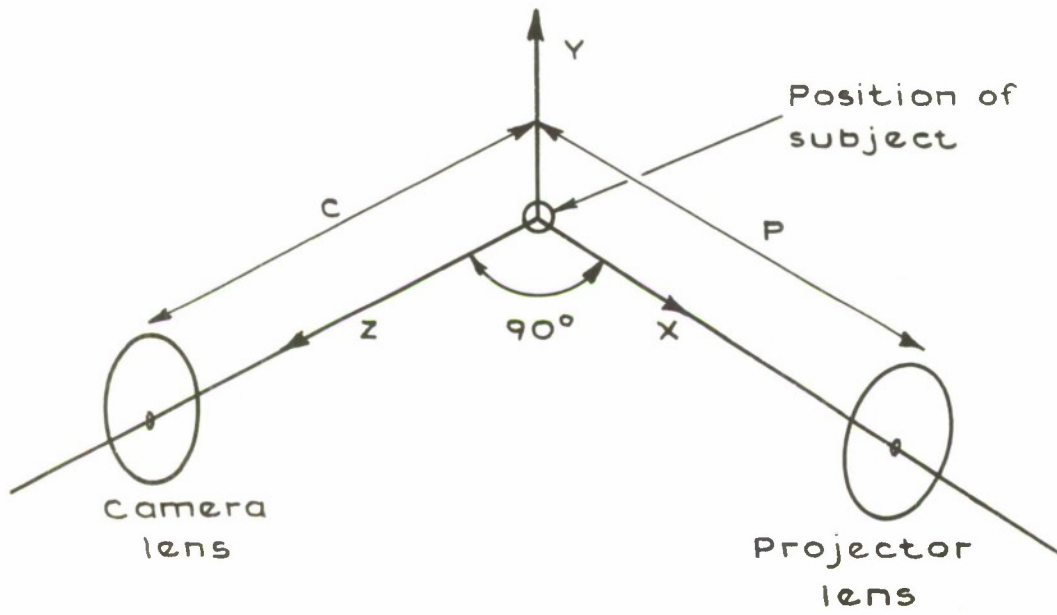


Fig. 2 Takasaki's Moiré method



TR 71184

054 900672

Fig.3 System of axes for contouring equipment

Fig.4

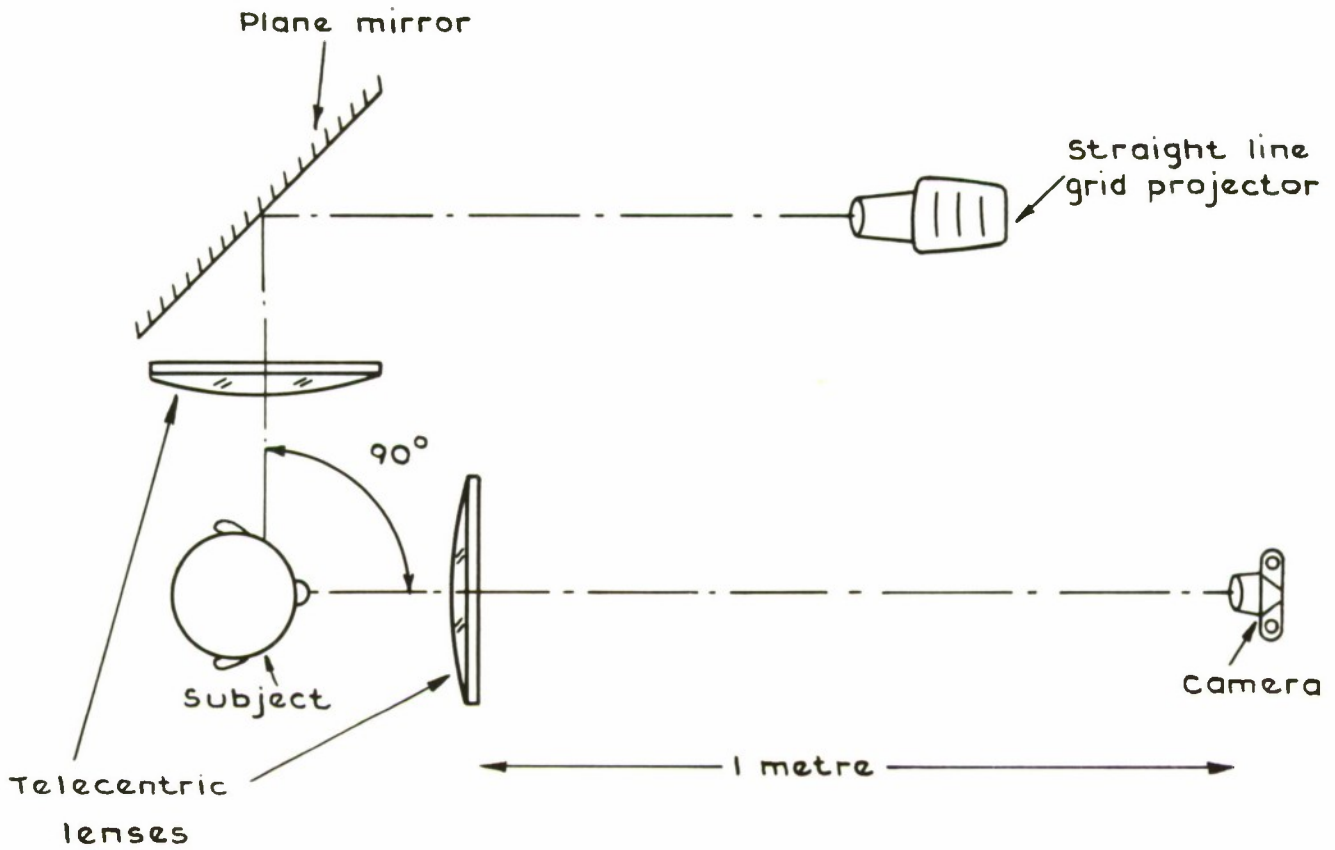
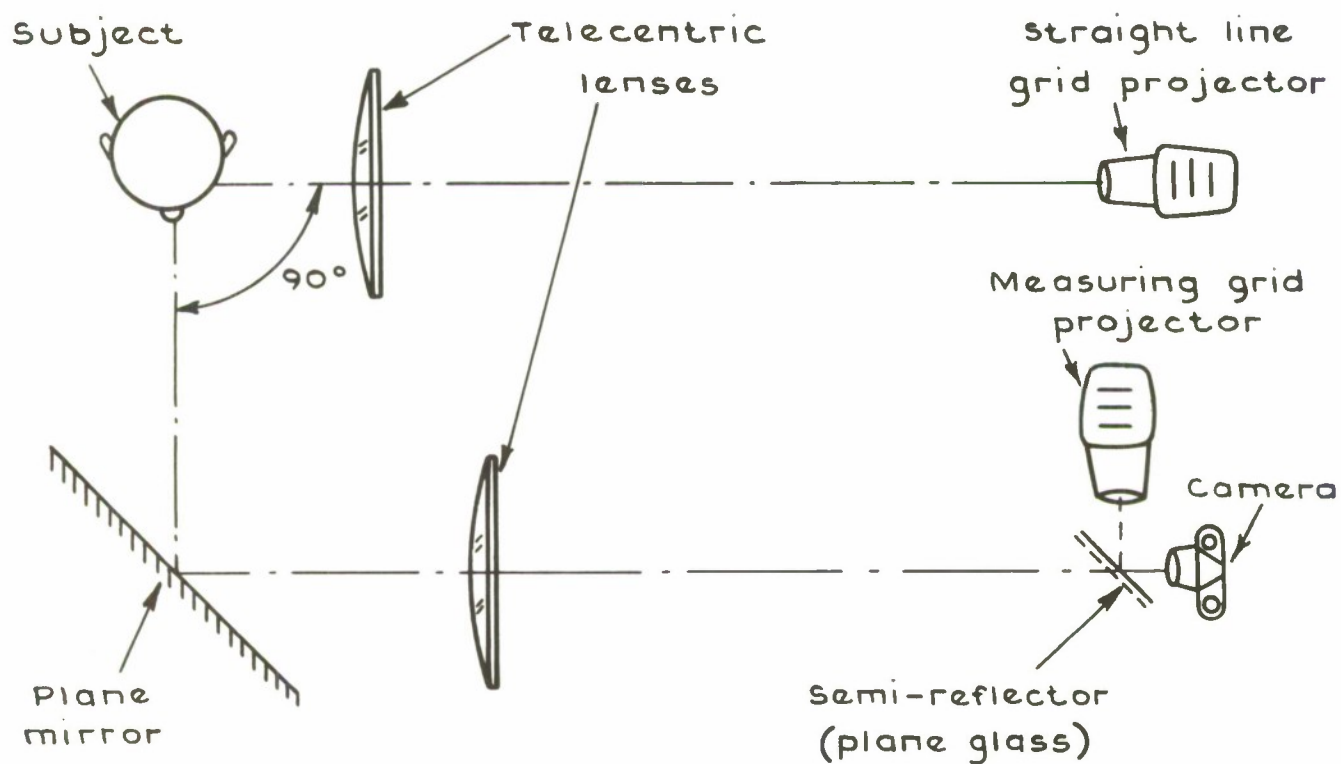


Fig.4 Plan view of telecentric system

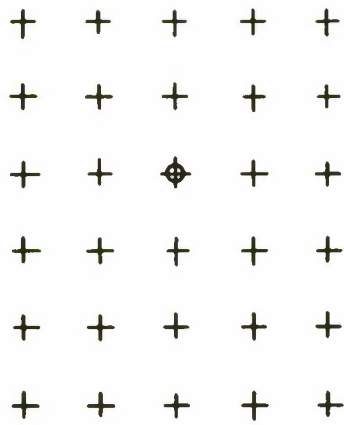


TR 71184

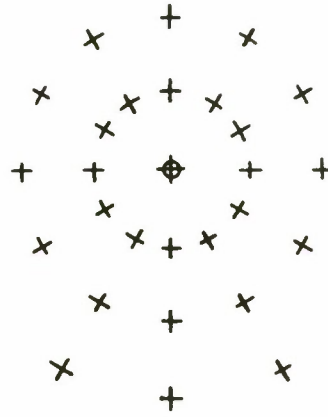
054 900874

Fig. 5 Telecentric system with measuring grid

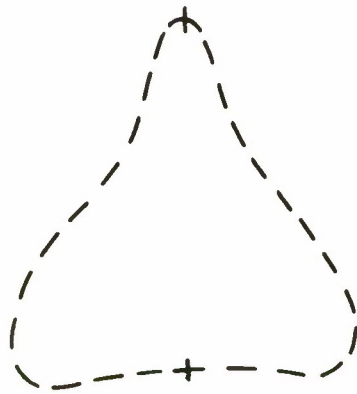
Fig. 6 a-c



a Rectangular

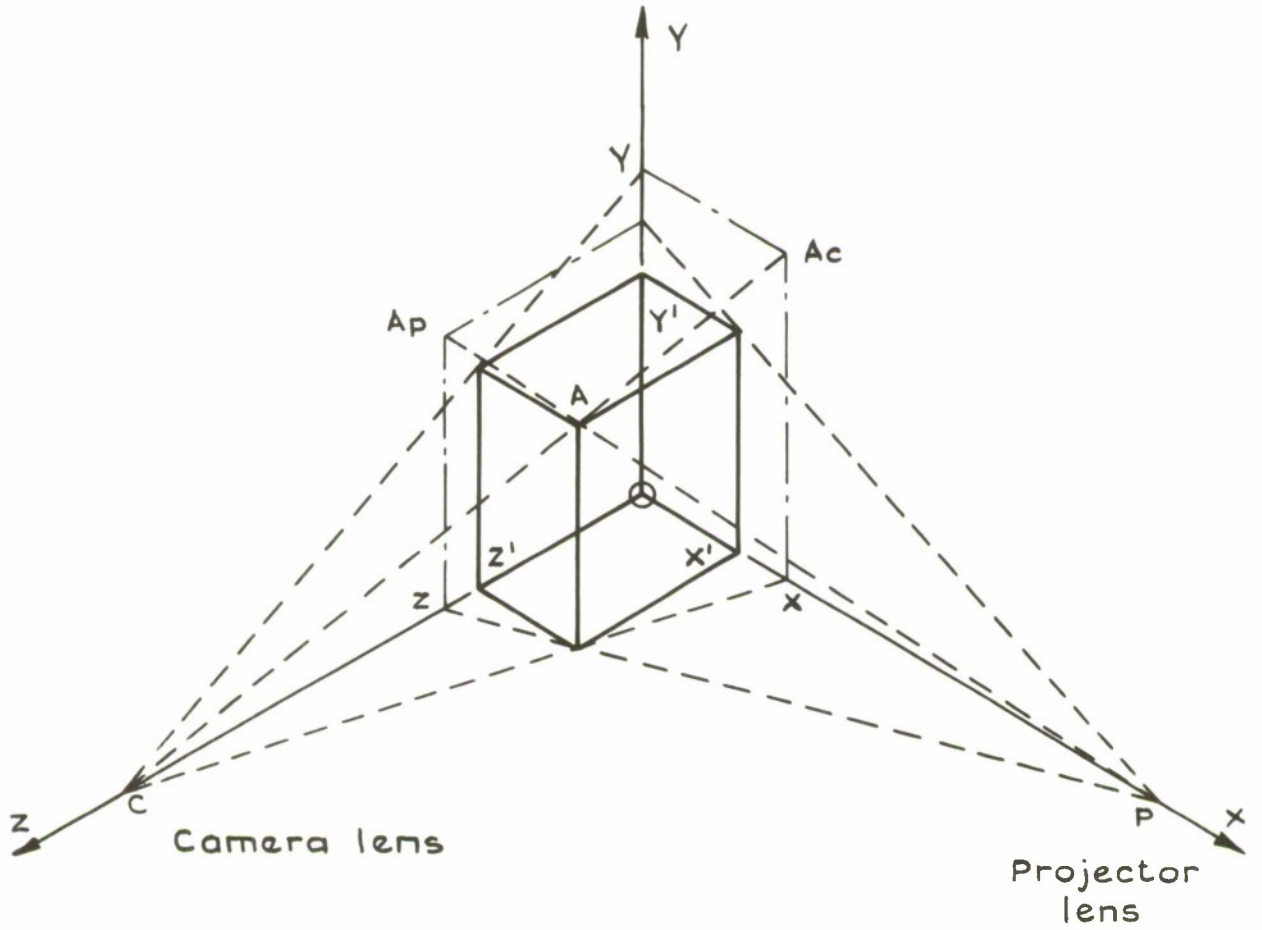


b Polar



c Mask outline

Fig. 6 a-c Measuring grids (seen as white against the coloured contours)



TR 71184

054 900876

Fig . A1 Apparent position of a general point 'A'

Fig. B1 & B2

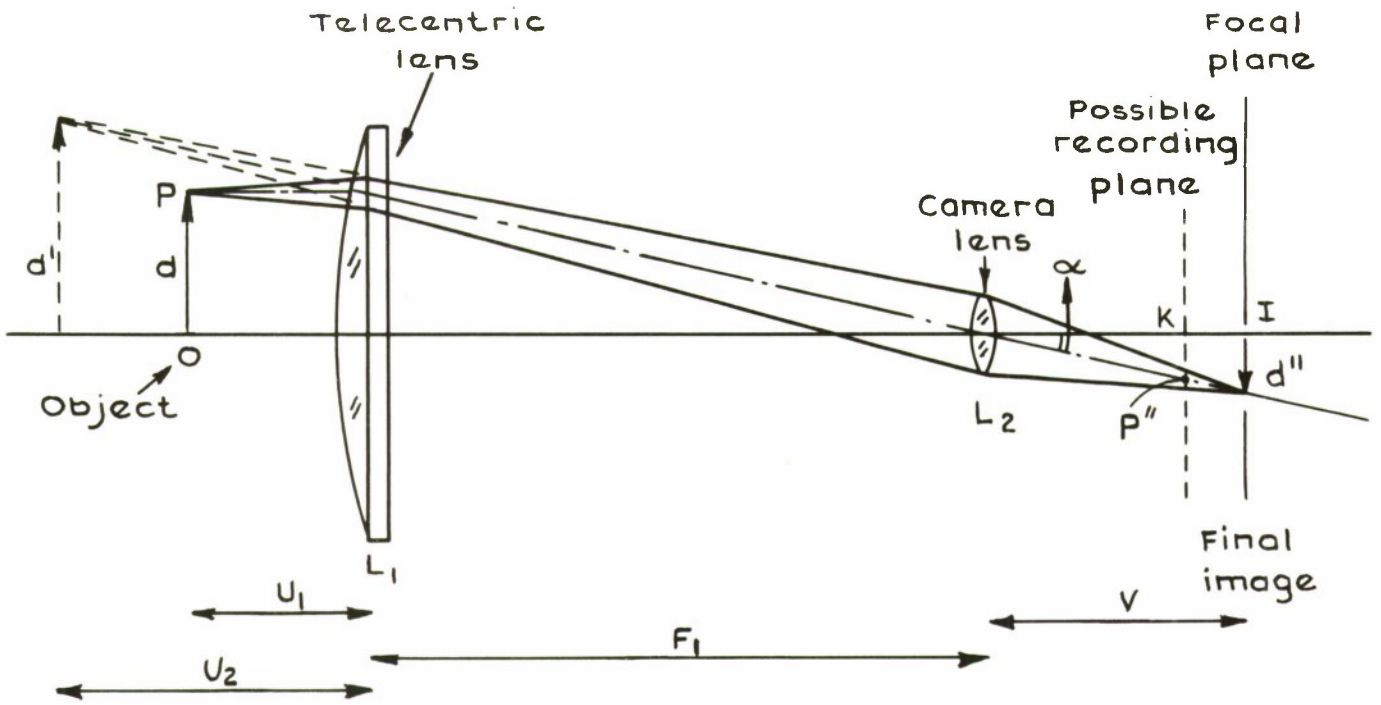


Fig. B1 Magnification on the film by telecentric system.

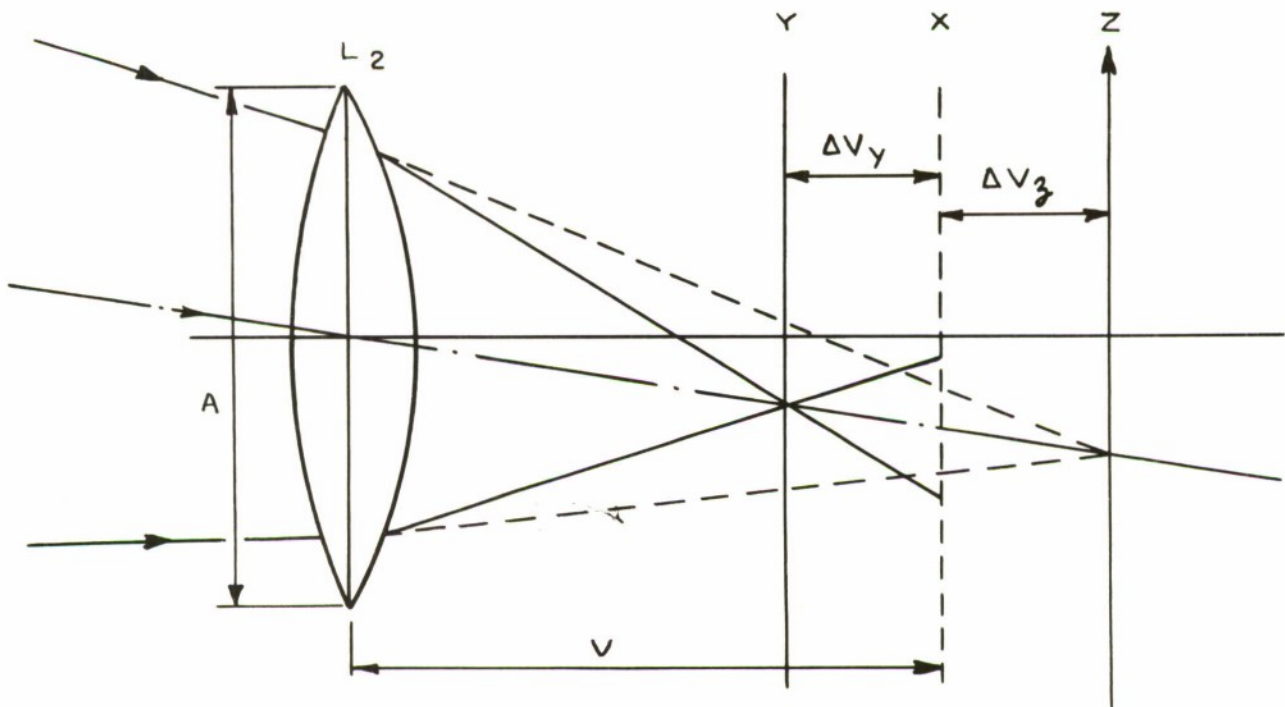
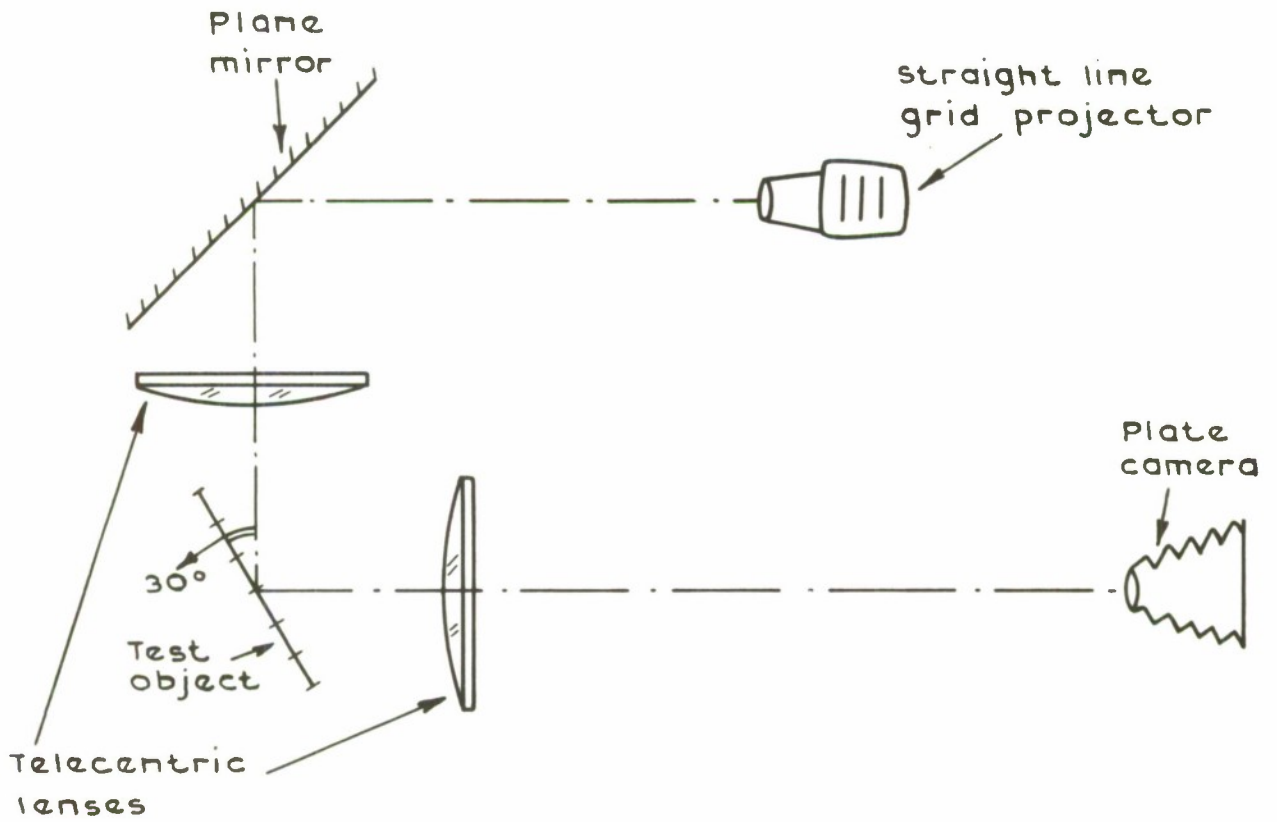


Fig. B2 Depth of focus of telecentric system



• TR 71184

054 900878

Fig.C1 Test set-up for telecentric system

Fig.C2 & C3

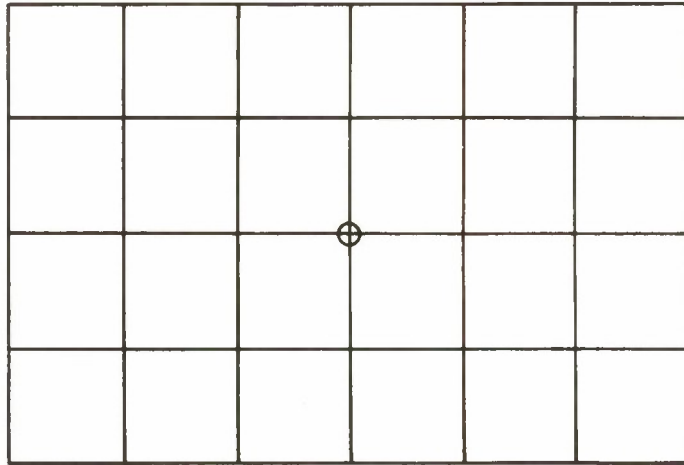


Fig.C2 Test object – flat plate marked in
50mm squares (35 points)

X Y Z		+0.14	+0.32	+0.03	-0.38	-0.91		
		+0.12	+0.12	+0.35	-0.23	-0.82		
		+0.43	+0.06	+0.08	+0.11	-0.27		
		+0.55	-0.56	-0.15	+0.14	+0.32	-0.21	-1.67
		-0.33	+0.14	+0.61	+0.49	+0.49	+0.14	-0.45
		+0.21	-0.16	-0.14	+0.28	+0.30	-0.07	-0.24
	+0.90	-0.44	-0.03	+0.03	+0.32	+0.26	-0.73	
	-0.31	-0.08	-0.08	+0.16	+0.28	+0.04	-0.19	
	-0.38	-0.16	-0.14	+0.08	+0.30	+0.13	+0.15	
	+0.55	-0.21	-0.03	+0.38	+0.43	+0.26	-0.97	
	+0.06	-0.17	-0.29	-0.17	-0.29	-0.17	+0.06	
	+0.01	-0.16	-0.14	+0.08	+0.30	+0.13	-0.24	
		+0.14	+0.44	+0.38	+0.67	+0.03		
		-0.03	-0.15	-0.15	+0.20	+0.67		
		+0.04	-0.14	-0.12	+0.11	-0.46		

Table C3 Error chart of test object (correct figure) –
(photograph figure) in mm

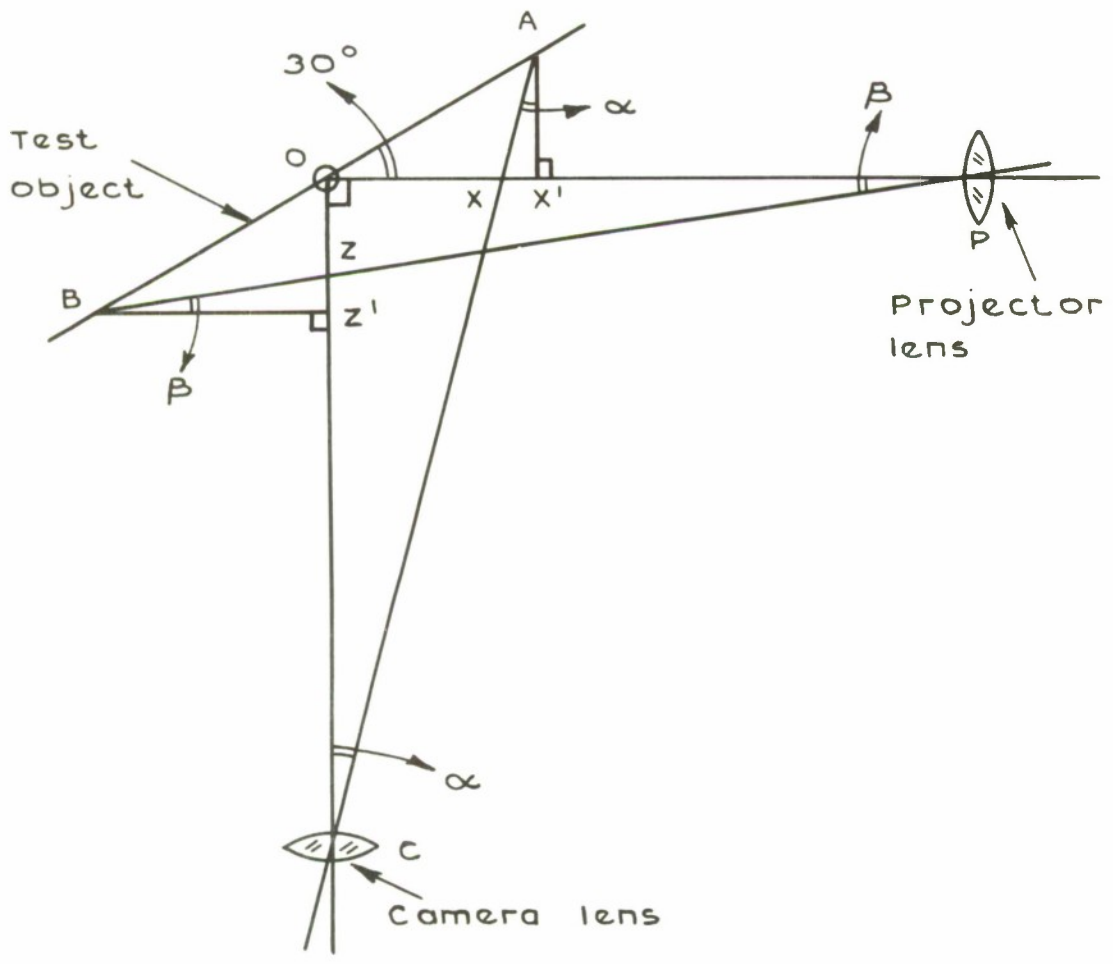


Fig.D1 Inaccuracies involved in a non-telecentric system (X and Z)

• TR 71184

054 900860

